

Marine Meteorology for Multi-Mega-Watt Turbines

Jens Tambke¹, Lorenzo Claveri², John A.T. Bye³, Carsten Poppinga¹,
Bernhard Lange⁴, Lueder von Bremen¹, Jörg-Olaf Wolff⁵

¹ForWind - Center for Wind Energy Research,
Institute of Physics, University of Oldenburg, 26111 Oldenburg, Germany
e-mail: jens.tambke@mail.uni-oldenburg.de, Tel. +49-441-36116736, www.energiemeteorologie.de

²FMI, Finnish Meteorological Institute, Helsinki, Finland

³School of Earth Sciences, The University of Melbourne, Victoria 3010, Australia

⁴formerly ¹ForWind, now ISET e.V., University of Kassel, 34119 Kassel, Germany

⁵Physical Oceanography (Theory), ICBM, University of Oldenburg, 26111 Oldenburg, Germany

Abstract

To achieve precise wind resource assessments, to calculate loads and wakes as well as for reliable short-term wind power forecasts, the vertical wind profile above the sea has to be modelled with high accuracy for tip heights up to 160m. For these purposes, it is crucial to consider the special meteorological characteristics of the marine atmospheric boundary layer. Continuing our work in the EU-project ANEMOS, we analysed marine wind speed profiles that were measured at the two met masts Horns Rev (62m high) and FINO1 (100m) in the North Sea. We found pronounced effects of thermal stratification and of the influence of the land-sea transition. In many situations, the wind shear is significantly higher than expected with Monin-Obukhov corrected logarithmic profiles. As a consequence, the standard approaches to calculate wind speeds in higher altitudes from given lower level values would lead to severe underestimations, especially for high Multi-Mega-Watt turbines.

For that reason, we developed a new analytic model of marine wind velocity profiles. In particular, the flux of momentum through the Ekman layers of the atmosphere and the sea is described by a common wave boundary layer. The good agreement between our theoretical profiles and observations at Horns Rev and FINO1 support the basic assumption of our model that the atmospheric Ekman layer begins at 15 to 45 m height above the sea surface. Moreover, we used the observations at Horns Rev, FINO1 and two lightships to evaluate numerical weather re-analysis data of the marine wind field above the North Sea.

Key words: Offshore Wind Resource Assessment; Wind Power Prediction, Wind Speed Profile; Ekman Layer

1. Introduction

In contrast to profiles over land the meteorological situation offshore is different mainly due to three important effects:

- 1) The non-linear wind-wave interaction leads to a variable, but small surface roughness.
- 2) The large heat capacity of the water strongly affects the thermal stratification of the air.
- 3) Internal boundary layers caused by the land-sea discontinuity modify the marine atmospheric flow.

Previous investigations for sites in the Baltic Sea showed that these meteorological conditions over the sea strongly influence offshore wind profiles [2,3]. However, the wind conditions above the North Sea are expected to differ from those of the Baltic Sea owing to the long fetches, i.e. to the large distances to the nearest coast in most wind directions. In order to develop a more suitable model to describe the marine boundary layer, we introduce a new approach to derive a wind profile which explicitly considers the wind-wave interaction and the Ekman layer.



Figure 1: Satellite image of the North Sea, showing the positions of the FINO1 and Horns Rev measurement sites

2. Offshore wind profiles measured at Horns Rev

The meteorological mast at Horns Rev is located approximately 18km west of Blaavands Huk at the Danish North Sea coast and is operated by Elsam Engineering A/S [4]. We investigated the period from 10/2001 till 04/2002 for which the wind speed measurements in four heights (15m, 30m, 45m and 62m) are available. Air temperatures were measured at 13m and 55m above, the water temperature at 4m below the mean sea level (DNN). The measurement data is provided by the Database on Wind Characteristics (www.winddata.com). The data set contains about 23 000 records of 10-minute mean values.

In order to correct the wind speeds at 15m, 30m and 45m for flow distortion of the lattice mast, we applied a linear correction model developed by Hoejstrup [5]. To determine the correction coefficients, we analysed the wind speed ratios of the two cup anemometers on each side of the mast depending on the wind direction. The effect of dynamic pressure directly in front of the mast is modelled by a correction factor $u(\text{measured})/u(\text{undisturbed})=0.993$, whereas the maximum overspeeding near the wake of the mast leads to a factor of 1.041. From the two installed anemometers the one in front of the mast (according to wind direction) was selected for the following investigations.

In the first half of the given period, the water temperature is on average higher than the air temperature, whereas it is vice versa in the second half. Therefore, all thermal situations can be expected to occur. There was no information available on the accuracy of the calibration of the temperature sensors at 13m and 55m. Thus, it is uncertain whether a potential temperature difference close to zero, i.e. in the range -0.05 to $+0.05$ Kelvin, really denotes neutral conditions of the thermal stratification. For that reason, we considered all observed thermal situations.

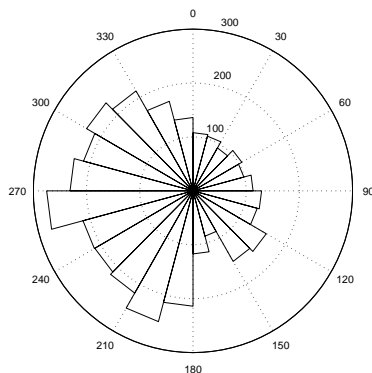


Figure 2: Frequency of wind directions in 43m height at Horns Rev in arbitrary units. Main wind directions: westerly winds from sea to land; Winter period 10/2001 till 04/2002

2.1 Dependence on wind direction

At Horns Rev, winds are mainly coming from the open North Sea with fetches of several hundred kilometres (Figure 1 and Figure 2).

In Figure 3 and Figure 4 the average profiles for different wind directions are shown. As expected the highest wind speeds are observed for the two sectors where the wind blows from westerly directions over the open sea, i.e. 225° to 315° . In these cases the strong winds generated by typical low pressure systems are not decelerated by land masses. In contrast to this, north-easterly winds (0° - 90°) which are mostly due to high pressure systems related to low wind speeds approach the site via the mainland of Denmark. Consequently, the corresponding measured profiles have considerably lower wind speeds. Finally, southerly and north-westerly winds (90° - 225° and 315° - 360°) have medium wind speeds.

Note that the height in Figure 3 and Figure 4 is plotted in a logarithmic scale. The standard logarithmic profile which would be expected in neutral situations would appear here as a straight line. In most sectors the measured profiles deviate from a logarithmic shape by higher wind shears. The supralogarithmic deviations are most pronounced for the five sea sectors with purely marine winds from the west (135° - 360°) where the profiles seem to be logarithmic up to 45m, but at 62m the measured wind speed is on average about 0.3 m/s higher than it would be estimated by a logarithmic extrapolation from the lower heights.

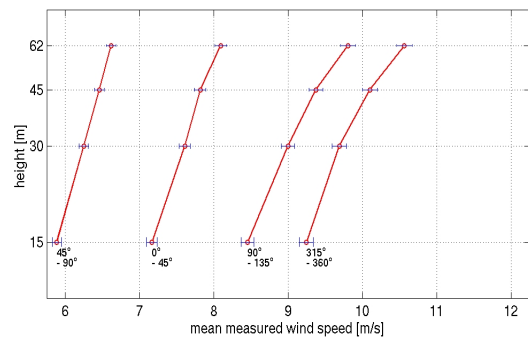


Figure 3: Mean measured profiles at Horns Rev for different northerly and easterly wind directions from 315° to 135° . Logarithmic scale of height.

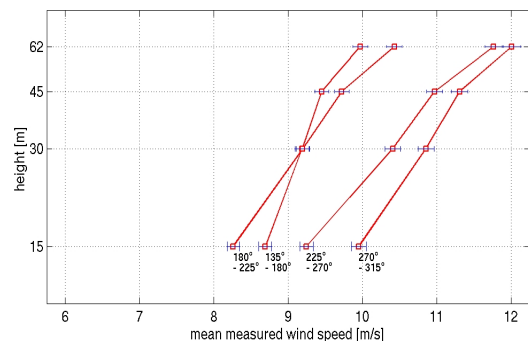


Figure 4: As Fig. 3, but for different southerly and westerly wind directions from 135° to 315° .

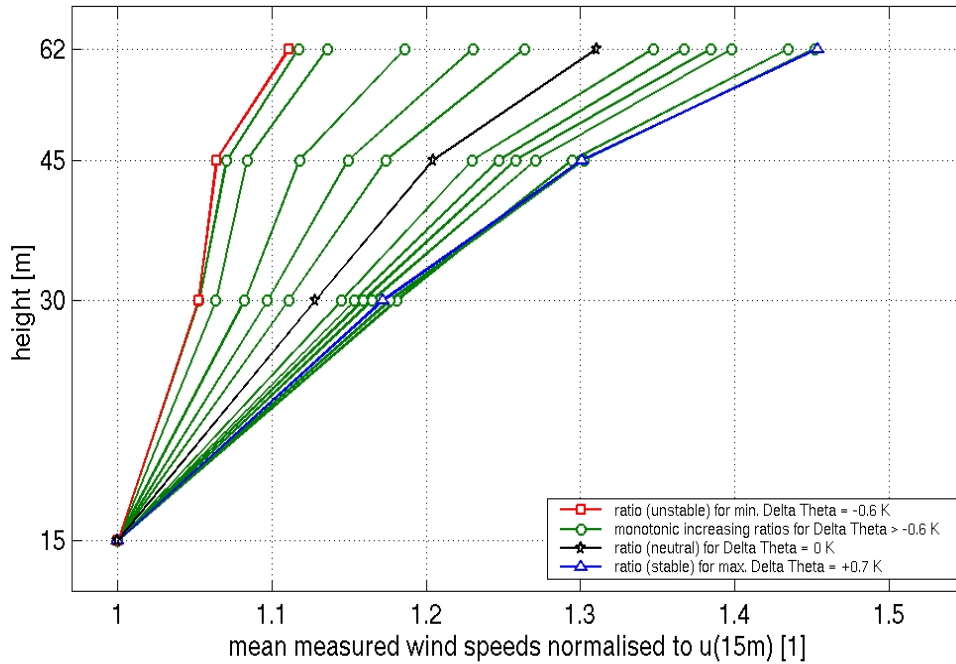


Figure 5: Relative mean measured wind speed profiles normalised to the speed at 15m height, for the wind speed bin of 9.5m/s to 10.5m/s at 30m height and wind directions from 135° to 360°, showing all observed potential temperature differences from $\Delta\theta = -0.6K$ (small gradients of wind speed) in steps of 0.1K up to $\Delta\theta = +0.7K$ (high gradients) with monotonically increasing speed ratios. Logarithmic scale of height

2.2 Dependence on thermal stratification

These supralogarithmic deviations could be easily explained with a stable thermal stratification of the boundary layer. But remarkably, this ‘bending’ to higher wind speeds at 62m height occurs in all thermal conditions that were observed at Horns Rev: Figure 5 shows the normalised mean measured wind profiles from the sea sectors for the complete range of observed potential temperature differences $\Delta\theta$ (from -0.6 K to +0.7 K) between 13m and 55m height. These profiles belong to a wind speed bin of 9.5 m/s to 10.5 m/s at 30m height.

All other wind speed bins show the same characteristics. The ‘bending’ even for clearly unstable conditions cannot be explained with a logarithmic profile corrected with Monin-Obukhov similarity theory. Besides this striking feature, the wind speed gradients follow the expectations for different thermal stratifications: Unstable conditions are related to small gradients and stable conditions to high gradients.

Deviations of offshore profiles from the logarithmic profile caused by internal boundary layers (IBL) related to the land-sea discontinuity have been observed for sites in the Baltic Sea [6]. But this is no explanation for the sea sector profiles at Horns Rev as the fetches of 500 to 800km seem to be far too long for this sort of IBL to sustain.

The observed effect of supralogarithmic measured wind speeds at heights above 45m might have physical reasons owing to the meteorological conditions at sea. In particular, the height of the surface layer might be decreased such that the

logarithmic wind profile loses its validity in lower heights compared to onshore and the anemometers at 30m and 45m height already probe the Ekman layer.

In contrast to this, it is possible that the applied correction for flow distortion due to the lattice mast is not sufficient. Therefore, we looked for a direction dependency of the deviations by comparing small sectors ($\pm 15^\circ$) around the wind direction where the mast is directly behind the anemometer to directions where the anemometers are besides the mast. In all cases the profiles show the same difference from the logarithmic shape. In addition, measurements carried out on a mast of the same type located at Læsø wind farm in the Baltic Sea and also operated by ELSAM do not show an increased wind speed recorded on top of the mast [4]. Hence, a systematic error due to the geometry of the mast is not detected. Nevertheless, the possibility remains that the observed “supralogarithmic bending” is an artefact of the measurement procedure.

However, the thermal stratification has an important impact on the flow for all wind speeds: As to be expected, the wind speed ratios between 62m and 15m increase with increasing thermal stability of the flow, classified by the gradient Richardson number Ri_g . The accuracy of the measurements does not support a calculation of the Monin-Obukhov-Length L . But the increase, from ratios of 1.1 (convective situations) to 1.6 (stable situations), is steeper than normally observed onshore (Figure 6). Similar results were found by Lange [2] for the Baltic Sea, but with relatively small fetches to the coastline (10-50 km).

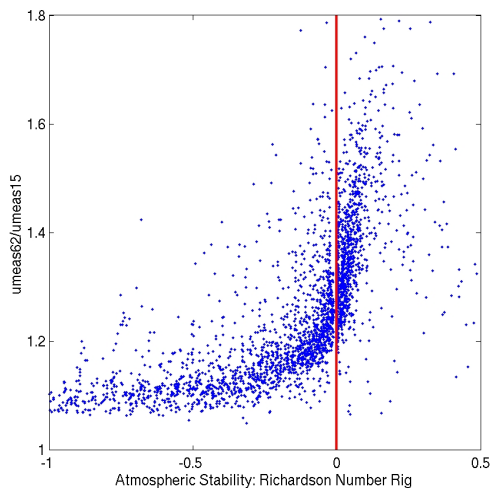


Figure 6: Ratios between measured wind speeds at 62m and 15m height depending on the gradient Richardson Number Rig as a measure of thermal stability of the atmospheric flow at Horns Rev.

2.3 Comparison with FINO1 profiles

The FINO1 measurement platform [7] is located 45km north of the island of Borkum in the North Sea (see Fig. 1). Eight cup anemometers are installed at heights of 30m to 100m, those from 30m to 90m on booms mounted in south-east direction of the mast. Three ultrasonic anemometers are present at heights of 40m, 60m, and 80m on north-westerly oriented booms. Additional meteorological measurements consist of wind direction, air temperature, moisture, air pressure and solar irradiation. Data from January to December 2004 have been used in this study. The data set contains about 70.000 records of 10-minutes average values.

The first results support the Horns Rev findings of supralogarithmic wind shears for westerly winds (180°-270°) for all thermal stratifications, but the effect of the mast for other wind directions could not be completely corrected yet.

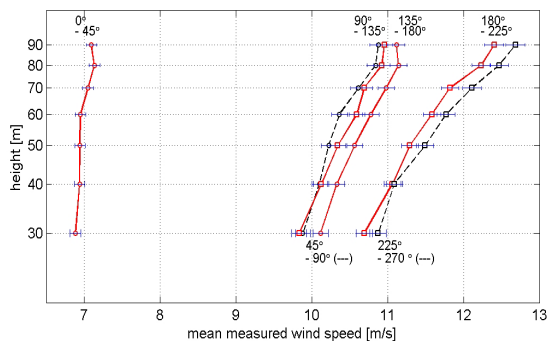


Figure 7: Mean measured profiles at FINO 1 for different wind directions from 0° to 270° (only 5 months data). Logarithmic scale of height.

Ultrasonic anemometer measurements are utilized to derive fluxes and determine the atmospheric stability. At FINO 1, a 3-dimensional calibration is applied to reduce the measurement error of the ultrasonic anemometers [8]. The planar fit method is used for tilt correction and linear regression for trend removal before momentum and heat fluxes are calculated with the eddy-correlation method. The Monin-Obukhov length L is derived from these fluxes. The wind speed profile in the atmospheric surface layer is commonly described by Monin-Obukhov theory. In homogenous and stationary flow conditions, it predicts a log-linear profile:

$$u(z) = \frac{u_*}{\kappa} \left[\ln\left(\frac{z}{z_0}\right) - \Psi_m\left(\frac{z}{L}\right) \right]$$

The wind speed u at height z is determined by friction velocity u_* , aerodynamic roughness length z_0 and Monin-Obukhov length L . κ denotes the von Karman constant (taken as 0.4) and Ψ_m is a universal stability function. The Businger-Dyer formulation [9] of the stability function with parameters of the reanalysis by Högström [10] are used.

If the wind speed is known at one height, the vertical wind speed profile is determined by two parameters: the surface roughness z_0 and the Obukhov length L . Here, a constant roughness of $z_0=0.0002\text{m}$ and the Obukhov-length calculated from the ultrasonic anemometer at 40m height are used.

A comparison of the measured wind shear with the predictions of Monin-Obukhov theory is made by plotting the measured wind speed ratio at two heights versus stability parameter $10\text{m}/L$. Here the heights of 50m and 30m were chosen. Only records with wind speeds above 5 ms^{-1} have been used to avoid increased scatter.

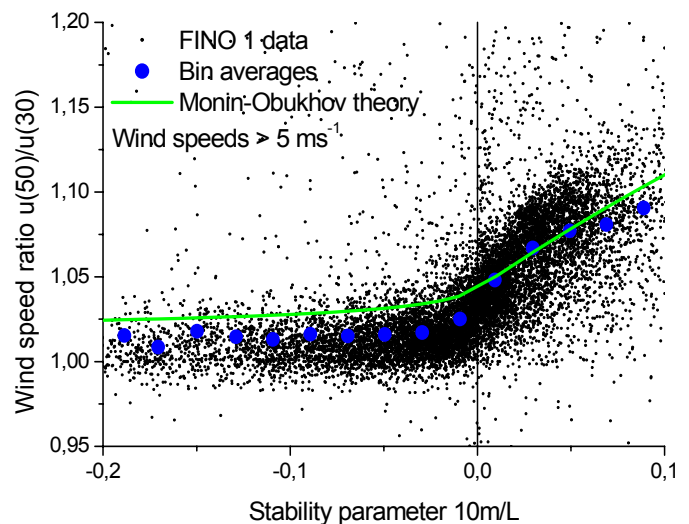


Figure 8: Measured wind speed ratio (wind shear) between the wind speeds at 50m and 30m height versus stability parameter $10\text{m}/L$ for the FINO 1 site

Figure 8 shows the measured data of the FINO I station, their bin averages and the prediction of Monin-Obukhov theory. A large scatter can be seen in the measurement data. This is caused by two effects:

- Instationary flow situations, where a relation between wind shear and stability can not be expected.
- Large sampling variability of covariance measurements at a relatively high altitude and with an averaging period of only 10 minutes.

It can be seen that the measurements show systematically lower wind shear than the theory for unstable conditions, while for stable stratification the agreement is better, but not satisfying.

3. Theory of inertially coupled wind profiles

In this section we follow the idea that physical reasons let the offshore wind profiles deviate from the standard expectations. We present an alternative vertical wind profile model that is based on inertial coupling between the Ekman layer of the atmosphere and the currents of the sea introduced by Bye in [11] and [12]. It is beyond the scope of this paper to provide a full derivation of the underlying theory. Hence only a first and brief outline of the main ideas is given and details will be published later ([13], and J. Tambke *et al.*, 2005, *in preparation*).

As usual the geostrophic wind is regarded as the driving force of the wind field in lower layers of the atmosphere. The momentum is transferred downwards through the Ekman spiral which is defined by a constant turbulent viscosity [14]. Similar to the Ekman layer of the air there is an Ekman layer of the water below the sea surface.

The important point addressed here is to derive an adequate description of the coupling between the two Ekman layers where the idea is to introduce a wave-boundary layer with a logarithmic wind profile that reaches only up to a maximum of 30m. The momentum transport from the wind flow into the ocean and hence, the wind profile then crucially depend on the coupling relations between the three flow layers.

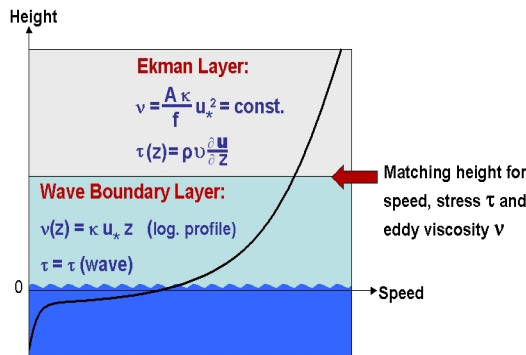


Figure 9: Scheme of the vertical wind profile used in the ICWP model.

3.1 Basic assumptions

In order to derive the coupling relations, the following assumptions are made.

First, close to the wave surface the ratio between the drift velocities of air, u_{air} , and water, u_{water} , is given by the square root of the density ratio of the two fluids. The same holds for the ratio between the friction velocities:

$$\frac{u_{water}}{u_{air}} = \frac{W_*}{u_*} = \sqrt{\frac{\rho_{air}}{\rho_{water}}} \quad (1)$$

where u_* is the friction velocity of the air flow and

W_* the one of water flow while ρ_{air} and ρ_{water} are the respective densities. This is equivalent to assuming that the shear stress is continuous across the interface between air and water.

The inertial coupling relation [11] determines this shear stress at the sea surface:

$$\tau(\text{wave}) = K_I (\sqrt{\rho_{air}} u_{air} - \sqrt{\rho_{water}} u_{water})^2, \quad \text{where } K_I \text{ is a drag coefficient.}$$

Second, the layer connecting the two Ekman layers of atmosphere and ocean is assumed to have a constant shear stress and will be denoted as wave-boundary layer extending from a height z_B above to $-z_B$ below the water level. This layer is similar to the surface layer onshore where the logarithmic wind profile is valid. Third, analogous to the similarity relation (1) the turbulent viscosities, ν_{air} and ν_{water} of the two Ekman layers are also assumed to be weighted according to the density ratio of the two fluids:

$$\frac{\nu_{water}}{\nu_{air}} = \frac{\rho_{air}}{\rho_{water}} \quad (2)$$

As shown by Bye [12] these physically justified conditions allow the determination of the velocities of the two fluids at certain heights dependent on a given geostrophic wind. The full profiles can then be derived in the following way.

Due to the constant shear stress the wind profile in the wave-boundary layer has a logarithmic shape. Expressed in a coordinate system where the horizontal component of the stress tensor $\vec{\tau}_h$ is parallel to the x-axis the profile can be written as

$$\vec{u}(z) = \left(u_L + \frac{u_*}{\kappa} \ln\left(\frac{z}{z_R}\right), \nu_L \right) \quad (3)$$

and is valid for $z_R \leq z \leq z_B$. κ is the von Karman constant and z_R is the height where the momentum transfer from the air to the wave field is centred. Because of the above assumptions and the choice of the coordinate system the 'offset' (u_L, ν_L) is directly

given by the geostrophic wind $\vec{G} = (u_g, v_g)$ [12]:

$$(u_L, v_L) = \frac{1}{2} \vec{G} \quad (4)$$

Note that in the chosen coordinate system $u_g > 0$ and $v_g < 0$.

The relation that connects the friction velocity u_* at the water surface to the geostrophic wind is given by

$$|\vec{G}| = \frac{\sqrt{r^2 + 1}}{|r + 1|} \frac{u_*}{\sqrt{K_1}} \quad (5)$$

where K_1 is the drag coefficient of the wave-boundary layer and the angle of rotation of the surface stress tensor to the left hand side of the geostrophic velocity (in the northern hemisphere) is $\text{atan}(-1/r)$ with $-1 < r < -\text{infinity}$; r has still to be determined.

The height of the wave-boundary layer z_B has to be related to the wave field. Previous results from oceanography suggest that z_B is reciprocal to the peak wave number, k_p , of the wave spectrum [15]. The corresponding peak wave velocity, c_p is given by $c_p = \sqrt{g/k_p}$ where g is the gravitational constant. Assuming that c_p is proportional to the wind speed $u(z_B)$, i.e. $c_p = B u(z_B)$, the height of the wave-boundary layer can be written as

$$z_B = \frac{B^2 (2r + 1)^2}{8g (r^2 + 1)} |\vec{G}|^2 \quad (6)$$

The factor B has been determined from empirical data by Toba [16]. For heights above z_B the velocity vector in the Ekman layer is described by an Ekman spiral

$$u(\hat{z}) = \hat{u}_1 [\cos(\beta\hat{z}) - \sin(\beta\hat{z})] e^{-\beta\hat{z}} + u_g \quad (7)$$

$$v(\hat{z}) = \hat{v}_1 [\cos(\beta\hat{z}) + \sin(\beta\hat{z})] e^{-\beta\hat{z}} + v_g \quad (8)$$

with $\hat{z} = z - z_B$ and $\beta = \sqrt{f/(2\hat{v})}$ where f is the Coriolis parameter, \hat{v} is the turbulent viscosity, $\hat{u}_1 = 0.5 u_g/r$ and $\hat{v}_1 = -0.5 v_g$.

At the interfaces between wave-boundary layer and Ekman layer, i.e. $z = \pm z_B$, the turbulent stress tensor and the turbulent viscosity is assumed to be continuous such that the wind profiles can be matched smoothly. This matching condition at the transition between wave-boundary layer and Ekman layer provides the necessary link to calculate the parameter r . At $z = z_B$ the height dependent viscosity

$$\nu(z_B) = K u_* z_B \quad (9)$$

of the wave-boundary layer and the constant viscosity

$$\hat{\nu} = \frac{2}{f} (r + 1)^2 K_1 u_*^2 \quad (10)$$

of the Ekman layer are set equal, i.e. $\nu(z_B) = \hat{\nu}$. Using equations (5) and (6) this provides the defining equation for r :

$$-|\vec{G}| \sqrt{K_1} \left(\frac{B}{4K_1} \right)^2 \left(\frac{f}{g} \right) \frac{(2r + 1)^2}{(r + 1)^3 \sqrt{r^2 + 1}} = 1 \quad (11)$$

The parameters $K_1 = 1.5 \times 10^{-3}$ and $B = 1.3$ can be obtained from oceanographic measurements [12,16,17], f and g are known constants at the desired location and the geostrophic wind \vec{G} as driving force can be chosen. Hence, equation (11) can be iteratively solved for r and the vertical wind profiles according to equations (3) and (7,8) can be calculated. These profiles will be denoted ICWPs.

3.2 Comparison with measurements at Horns Rev and FINO 1

The wind speed profiles according to ICWP theory are calculated such that the wind speeds at 30m height correspond to the measurement at that height. In *Figure 10* the mean measured sea sector wind profile (135°-360°) at Horns Rev and the corresponding mean of the ICWP profiles are compared. The semilogarithmic plot shows again that the measured wind speed at 62m is on average larger than expected by a logarithmic extrapolation using measured wind speeds from two heights. Taking into account that the only information given to the ICWP model is the wind speed at 30m, the mean wind shear is covered remarkably well. The increased wind speed at 62 m is almost captured ($\text{bias} = 0.1\text{m/s}$) which is related to the non-logarithmic shape of the ICWP due to the Ekman part of the profile (equation (7)). The remaining differences in the profiles indicate that the parameters used in calculating the ICWPs have to be optimised. In particular, the height z_B that marks the transition between wave-boundary layer and Ekman layer is a candidate to be adjusted. The mean z_B derived for the ICWP here is 8.1m which seems quite low. The root mean square error RMSE for the whole time series amounts to 6.1 % of the wind speed at 62m height. Because of the crucial influence of thermal stratification on the wind shears (*Figure 6* and *Figure 8*), the RMSE could be halved if the correct thermal stratification would be known.

Figure 11 shows the same comparison for FINO1. The relative RMSE of the ICWPs over the full time series is 5% at 90m height and 10% at 100m.

At both sites, the offshore WASP profile leads to underestimations of the wind shear.

These preliminary results are not satisfying and require further analysis of modelled and measured profiles, especially regarding thermal conditions and the corrections for mast flow distortion, which seem to be problematic, especially for 80m height.

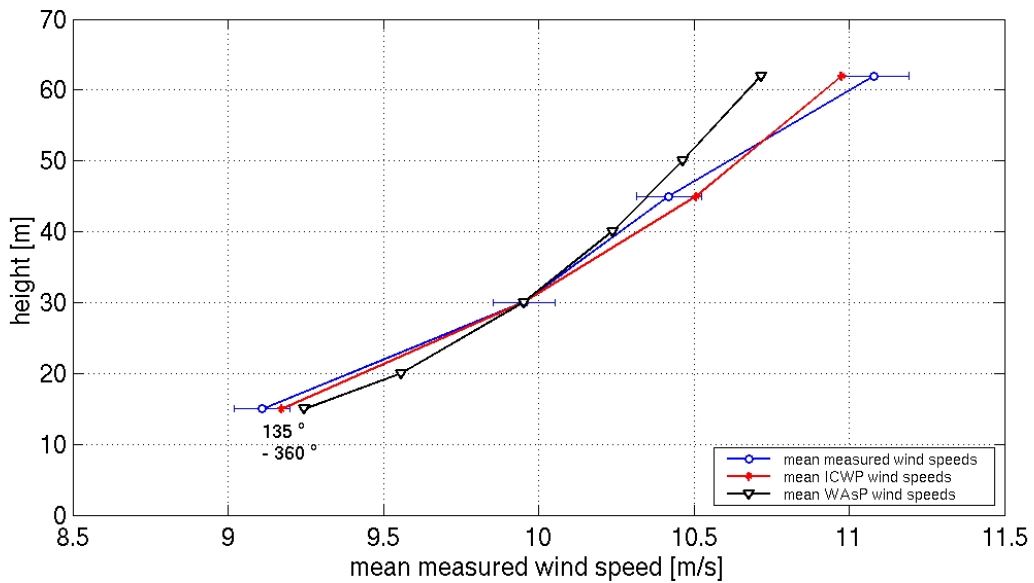


Figure 10: Mean measured “open sea” sector (135° - 360°) wind profile at Horns Rev compared to mean of ICWPs and average offshore WAsP profile.

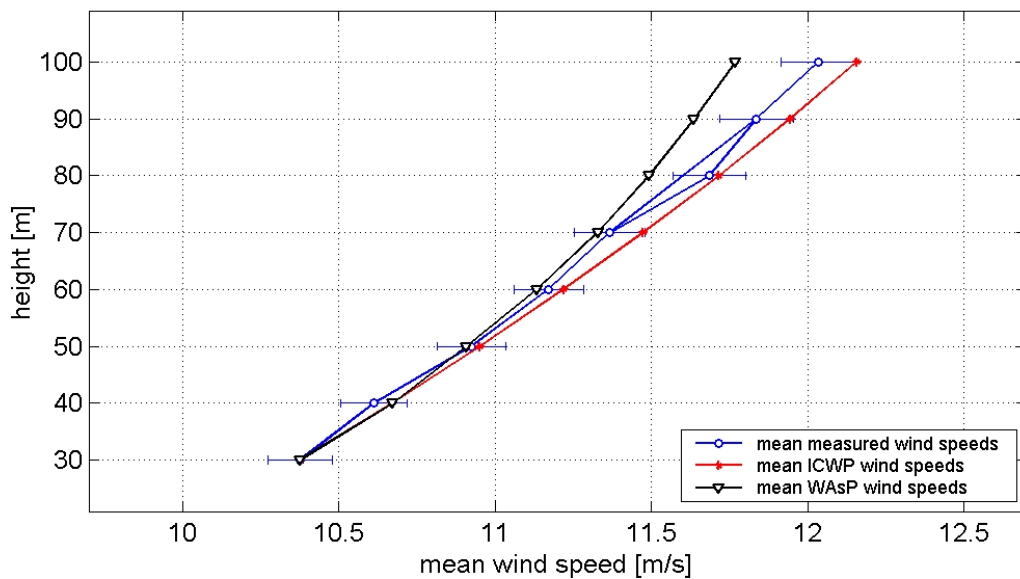


Figure 11: Mean measured “open sea” sector (190° - 250°) wind profile at FINO 1 compared to mean of ICWPs and average offshore WAsP profile.

4. Comparison of MM5 and DWD-Analysis at FINO1

Apart from the 1-dimensional micrometeorological analysis, we made a first evaluation of meso-scale-model simulations. Here we used the output of the German Weather Service (DWD) Analysis for the North Sea and our own MM5-simulation based on NCEP/NCAR Re-Analysis data. Figure 12 shows the same mean measured profile as Figure 11 (average in

year 2004), but compared to the mean profiles produced by the DWD-model and MM5 in that year for the wind direction sector 190°-250°. Both models reproduce the observed mean wind speed at 100m height, but show considerably lower wind shears than the measurement. But when evaluating the full time series at 100m, i.e. for the whole year 2004 and all wind directions, the MM5 simulation shows a mean 100m wind speed of 9.3m/s, whereas the DWD reproduces the mean measured wind speed of 9.8m/s.

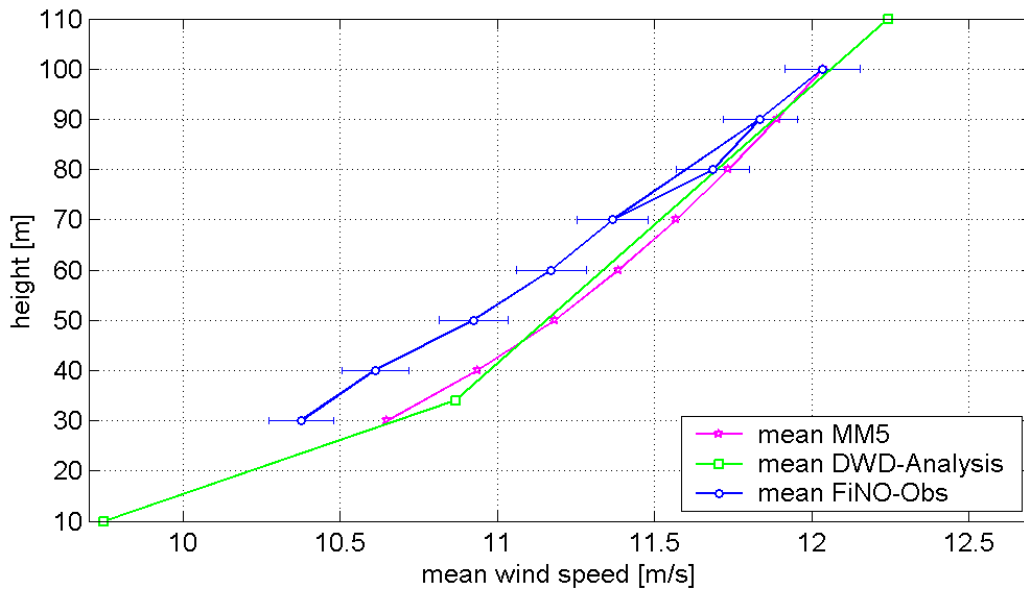


Figure 12: Mean measured sea sector ($190^{\circ} - 250^{\circ}$) wind profile at FINO1 compared to the mean output of two meso-scale simulations for the same wind directions: DWD-Analysis and MM5-Simulation (based on NCEP/NCAR Reanalysis).

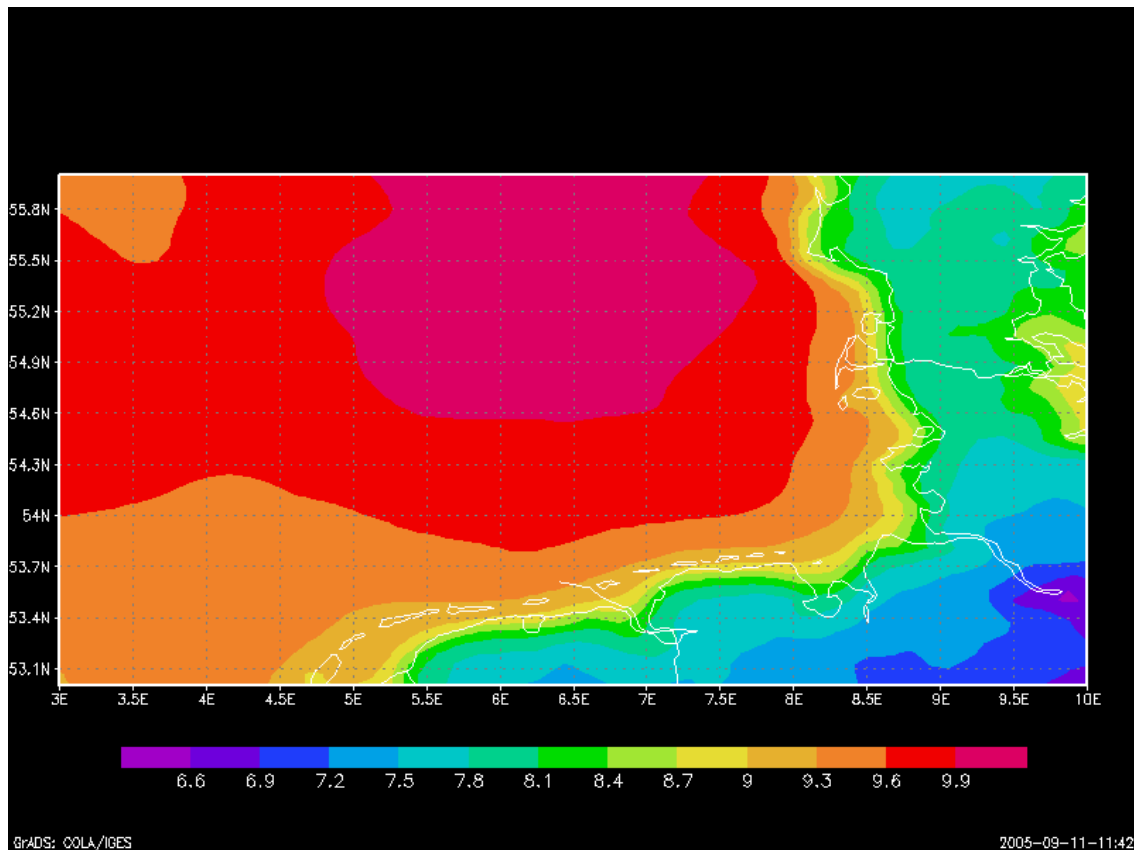


Figure 13: Mean 100m wind speeds in the German Bight in 2004, calculated from the DWD-Analysis.

The most important difference in the accuracy of both model outputs is the root mean square error: MM5 shows an RMSE of 2.5m/s against the observed time series at FINO1, DWD has an RMSE of only 1.4m/s.

Figure 15 shows that the BIAS and the STDBIAS (difference of standard deviations of both time series) of the DWD-Analysis are very small. The RMSE is fully determined by the dispersion (phase) error.

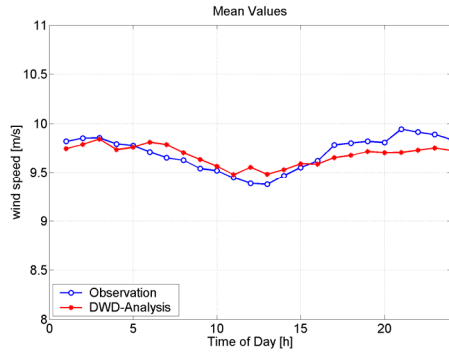


Figure 14: Mean 100m wind speeds at FINO1 for different times of the day, year 2004.

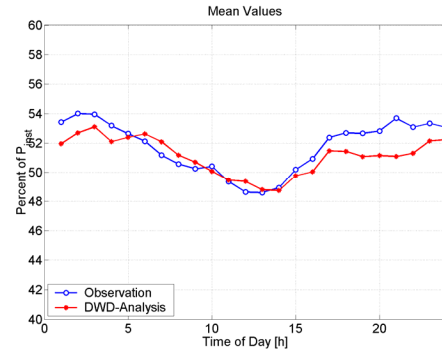


Figure 16: Mean calculated power output at FINO1 for different times of the day, year 2004.

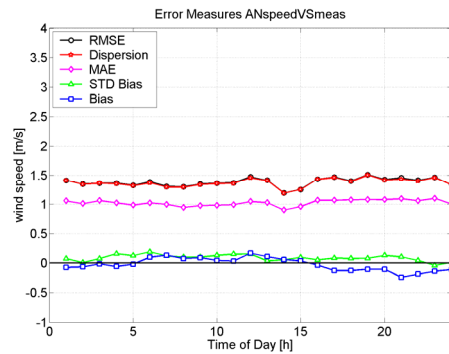


Figure 15: Error measures of wind speeds from DWD-Analysis against FINO1-Obs for different times of the day, year 2004.

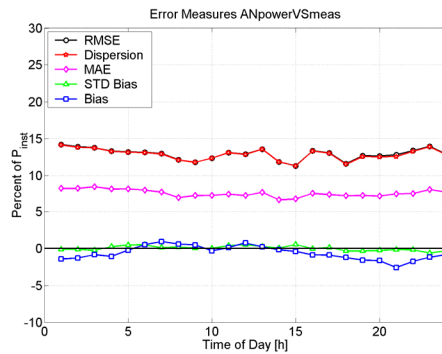


Figure 17: Error measures of calculated wind power from DWD-Analysis against FINO1-Obs for different times of the day, year 2004.

When we multiply the time series of wind speed with a typical multi-mega watt power curve, the mean diurnal variation of the wind speeds leads to a more pronounced variation of the mean power output between 48% and 54% of the installed capacity (Fig 16). The RMSE of the modelled power time series is 13% of the installed capacity (Fig17).

5. Conclusions

Our analysis shows that the offshore profiles measured at Horns Rev and FINO 1 deviate considerably from the expected shapes by higher wind shears. A meteorological reason might be found in a thinner logarithmic layer than onshore and a lower onset of the atmospheric Ekman layer. On the other hand, the possibility cannot be excluded that the effects are due to failures in the measurement process. Further investigations are necessary to confirm our findings.

We introduce an alternative way to describe the vertical wind profile over the sea which is based on inertially coupling the Ekman layers of air and sea with a wave-boundary layer with constant shear stress in between. For wind directions with long fetches the profiles derived by this method are in good agreement with the mean measured wind shears. In general, inertially coupled wind profiles (ICWPs) seem to be a promising approach with good potential

to be further improved. Future work has to focus on describing thermal air-sea interactions and fetch-dependent influences in order to improve both the description of wind profiles and the numerical prediction models, see [1,18]. Most important, thermal stratification has to be measured more precisely to allow a detailed modelling.

The wind speed Analysis of the German Weather Service seems to be a good candidate for a micrometeorological vertical refinement using the ICWP-theory in order to calculate the potential power output of future offshore wind farms.

6. Acknowledgements

We would like to thank www.winddata.com, Germanischer Lloyd, DEWI and DWD for providing the data. This work was funded by the European Commission (ANEMOS project, ENK5-CT-2002-00665) and the Hanse Institute for Advanced Study, Delmenhorst.

7. References

- [1] Tambke J. Forecasting Offshore Wind Speeds above the North Sea. *Wind Energy* 2005; **8**: 3-16.
- [2] B. Lange, S. Larsen, J. Højstrup, R. Barthelmie. Importance of thermal effects and sea surface roughness for offshore wind resource assessment. *Journal of Wind Engineering and Industrial Aerodynamics* **92** **11** (2004) 959-998
- [3] Watson SJ and Montavon C. CFD Modelling of the Wind Climatology at a Potential Offshore Farm Site. In *Proc. Europ. Wind Energy Conf. EWEC*, Madrid, 2003.
- [4] Sommer A. Techwise A/S. Offshore Measurements of Wind and Waves at Horns Rev and Læsø, Denmark. In *Preliminary edition for the OWEMES conference*, Naples, 2003.
- [5] Højstrup J. Vertical extrapolation of offshore wind profiles. In *Proc. Europ. Wind Energy Conf. EWEC*, pages 1220-1223, Nice, 1999.
- [6] Lange B. Modelling the Marine Boundary Layer for Offshore Wind Power Utilisation, *volume 491 of Fortschritt-Berichte VDI Reihe 6. VDI Verlag*, Düsseldorf, 2003.
- [7] Neumann T et al. One Year Operation of the First Offshore Wind Research Platform in the German Bight - FINO I. *German Wind Energy Conference DEWEK 2004*, Wilhelmshaven, Germany, 2004, published on CD
- [8] Tautz S, Lange B, Heinemann D. Correction of the heat and momentum flux measurements with the ultrasonic anemometers at the FINO I offshore meteorological mast for flow distortion and mounting effects. *German Wind Energy Conference DEWEK 2004*, Wilhelmshaven, Germany, 2004, published on CD
- [9] Businger JA, Wyngaard JC, Izumi Y, Bradley EF. Flux-profile relationships in the atmospheric surface layer. *Journal of the Atmospheric Sciences* **28** (1971) 181-189
- [10] Högström U. Non-Dimensional Wind And Temperature Profiles In The Atmospheric Surface Layer: A Re-Evaluation. *Boundary-Layer Meteorology* **42** (1988) 55-78
- [11] Bye JAT. Inertial coupling of fluids with large density contrast. *Phys. Lett. A*, **202**: 222-224, 1995.
- [12] Bye JAT. Inertially coupled Ekman layers. *Dyn. Atmos. Oceans*, **35**: 27-39, 2002.
- [13] Tambke J, Barthelmie R, Kariniotakis G et al. Description of Offshore Prediction Models. *Report D5.1 to the European Commission, ANEMOS Project*, <http://anemos.cma.fr>, November 20th, 2004
- [14] Ekman VW. On the influence of the earth's rotation on ocean currents. *Arkiv för Matematik, Astronomi och Fysik*, **2**: 1-53, 1905.
- [15] Jones ISF and Toba Y. Wind Stress over the Ocean. *Cambridge University Press*, Cambridge, 2002.
- [16] Toba Y. Local balance in the air-sea boundary process III. On the spectrum of wind waves. *J. Oceanor. Soc. of Japan*, **29**: 209-220, 1973.
- [17] Garratt JR. The atmospheric boundary layer. *Cambridge University Press*, Cambridge, 1992.
- [18] Tambke J, Poppinga C, von Bremen L, Claveri C, Lange M, Focken U, Bye JAT, Wolff J-O. Forecasting 25GW Wind Power above North and Baltic Sea. *Proc. Copenhagen Offshore Wind*, Copenhagen, 2005.